Simplified Stokes polarimeter based on division-of-amplitude

Negara, Christian, Li, Zheng, Längle, Thomas, Beyerer, Jürgen

Christian Negara, Zheng Li, Thomas Längle, Jürgen Beyerer, "Simplified Stokes polarimeter based on division-of-amplitude," Proc. SPIE 11144, Photonics and Education in Measurement Science 2019, 111441B (17 September 2019); doi: 10.1117/12.2532399

SPIE.

Event: Joint TC1 - TC2 International Symposium on Photonics and Education in Measurement Science 2019, 2019, Jena, Germany

Simplified Stokes polarimeter based on division-of-amplitude

Christian Negara[a], Zheng Li[a,b], Thomas Längle[a], and Jürgen Beyerer[a,b]

[a]Fraunhofer Institute of Optronics, System Technologies and Image Exploitation IOSB, Fraunhoferstr. 1, 76131 Karlsruhe, Germany
[b]Karlsruhe Institute of Technology, Kaiserstraße 12, 76131 Karlsruhe, Germany

ABSTRACT

A polarization state detector (PSD) measures the state of polarization of the detected light. The state of polarization is fully described by the Stokes vector containing four Stokes parameters. A division-of-amplitude photopolarimeter (DOAP) measures the four Stokes parameters by simultaneously acquiring four intensities using photodetectors. A key component of the DOAP is the first beam splitter, which splits up the incoming beam into two beams. The effect of the beam splitter on the state of polarization of the reflected (r) and transmitted (t) beam is determined by six parameters: $R, T, \Psi_r, \Psi_t, \Delta_r$, and Δ_t. R and T are the reflectance and transmittance, and (Ψ_r, Δ_r) and (Ψ_t, Δ_t) are the ellipsometric parameters of the beam splitter in reflection and transmission, respectively. To measure the Stokes vector with high accuracy, the six optical parameters must be chosen appropriately. In previous work, the optimal parameters of the beam splitter have been determined as $R = T = 1/2, \cos^2 2\Psi_r = 1/3, \Psi_t = \pi/2 - \Psi_r$, and $(\Delta_r - \Delta_t)$ modulo $\pi = \pi/2$ by calculating the maximum of the absolute value of the determinant of the instrument matrix. Using additional quarter-wave plates eliminates the constraint on the retardance and hence simplifies the manufacturing process of the beam splitter, especially when broadband application is intended. To compensate a suboptimal value of $\Delta_r - \Delta_t$, the azimuthal angles of the principal axes of the retarders must be adjusted, for which we provide analytic formulas. Hence, a DOAP with retarders is also optimal in the sense that the same values for the determinant and condition number of the instrument matrix are obtained. When using two additional retarders, it is necessary to mount both at the same light path in order to obtain an optimal DOAP. We will show that is also possible to get an optimal DOAP with only one additional quarter-wave plate instead of two, if one of the Wollaston prisms is rotated.

Keywords: polarimetry, ellipsometry, Stokes vector, polarization state detector, division-of-amplitude, beam splitter, retarder, quarter-wave plate

1. INTRODUCTION

The interaction of light and matter often results into a change of the state of polarization (SOP). This effect is used in many applications in industry, surface characterization, material science and thin film measurement.[1–6] Depending on the application, polarized or unpolarized light might be emitted. The measurement of the SOP is always a key component in applications using polarization-sensitive sensors. Polarization state detectors (PSD) measure the complete SOP, in contrast to incomplete polarimeters. The Stokes vector is a common notation to describe the complete SOP.

A PSD called division-of-amplitude photopolarimeter (DOAP) using only four intensity measurements to determine the Stokes vector has been proposed in the previous work.[7] It has no moving parts and the four intensity measurements are conducted simultaneously. Therefore, the DOAP is well suited for measuring the SOP at high sampling rates. The measurement error of the calculated Stokes vector can be assessed by the instrument matrix of the DOAP. Two quality measures are usually used to determine the measurement error of

Further author information: (Send correspondence to C.N.)
C.N.: E-mail: christian.negara@iosb.fraunhofer.de, Telephone: +49 (0)721 6091 567, Orcid: https://orcid.org/0000-0001-9649-6095
Z.L.: E-mail: zheng.li@iosb.fraunhofer.de, Telephone: +49 (0)721 6091 528
T.L.: E-mail: thomas.laengle@iosb.fraunhofer.de, Telephone: +49 (0)721 6091 212
J.B.: E-mail: juergen.beyerer@iosb.fraunhofer.de, Telephone: +49 (0)721 6091 210

Photonics and Education in Measurement Science 2019, edited by Maik Rosenberger, Paul-Gerald Dittrich, Bernhard Zagar, Proc. of SPIE Vol. 11144, 111441B
 · doi: 10.1117/12.2532399

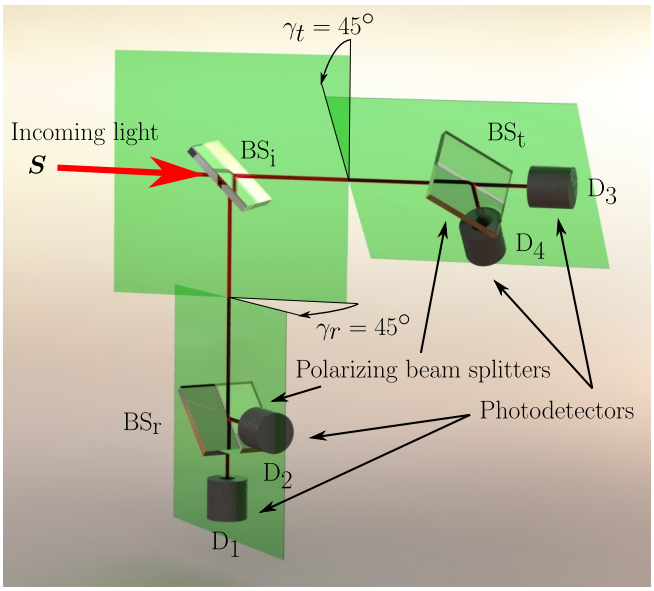

Figure 1. Scheme of the DOAP.

a PSD: the determinant and the condition number of the instrument matrix. We will show that both quality measures of the instrument matrix are simultaneously optimal.

The first beam splitter, which splits up the incoming light into two light beams, has a significant influence on the measurement error. Beam splitters consisting of optically isotropic media can be characterized by six optical parameters, if the plane of incidence remains unchanged while the light propagates through the beam splitter. The optical parameters of the DOAP must fulfill some constraints in order to achieve a low measurement error. These make the production of the beam splitter difficult, especially for broadband application, and in the end lead to higher production costs of the PSD.

In this article we will show how to simplify the production of the beam splitter by mounting additional quarter-wave plates while maintaining the optimality of the DOAP. This leads to a relaxation of the constraint on the retardance of the beam splitter. Quarter-wave plates with anti-reflection coatings ($T > 99.7\%$) are manufactured in bulk and are therefore cheaper than specially designed optical components*. Although the retardance is fixed to the quarter of a wave, rotating the quarter-wave plates has the same effect on the absolute value of the determinant as a variable retardance. Furthermore, we present a DOAP suited for broadband application and verify our calculations by using the physical optics software VirtualLab Fusion from LightTrans†.

2. PREVIOUS WORK

The measurement of the SOP can be performed in various ways e.g. by division-of-amplitude,[8] division-of-wavefront,[9] the four-detector photopolarimeter,[10] rotating compensators,[11] or liquid-crystals.[12] The focus of this article is restricted to the DOAP. A scheme of the DOAP is shown in Figure 1. The DOAP splits up the the incoming light beam into four linearly polarizes light beams with lower amplitude which are detected e.g. by four photodetectors. The first beam splitter BS_i splits up the incoming light beam into the reflected (r) and transmitted (t) beam. The DOAP has also two polarizing beam splitters, BS_r and BS_t, which split up the incoming light wave into two orthogonal linearly polarized waves. BS_r and BS_t could be e.g. Rochon prisms, Wollaston prisms, Nomarski prisms, Glan-Thompson prisms, or polarizing beam splitters like cubes or plates. The azimuthal angles of the polarizing beam splitters BS_r and BS_t are $\gamma_r = \gamma_t = 45°$.[8,13] We will use the Stokes-Mueller formalism[14,15] and the Nebraska ellipsometry conventions[16] to deal with the change of polarization of a light beam passing through polarizing optical elements. It is assumed that the diameter of the detectors is grater

*For example: Thorlabs zero-wave plate with article number WPQSM05-633
†https://www.lighttrans.com/

than the diameter of the incoming light beam. Otherwise, the relationship between the amplitude and intensity of a light beam at reflection and refraction[17,18] must be taken into account, when calculating the measured intensities with the Stokes-Mueller formalism.

The Stokes-Mueller formalism is used to calculate the instrument matrix depending on the parameters of the DOAP e.g. the optical parameters of BS_i. In this article, we analyse the influence of sensor noise on the calculation of the SOP by assessing the absolute and relative measurement error. A more accurate noise model consisting of an additive white Gaussian noise and Poisson noise has also been examined in previous work.[19] By maximizing the absolute value of the determinant of the instrument matrix, optimal values for the reflectance (R), transmittance (T), diattenuations (Ψ_r and Ψ_t), and retardances (Δ_r and Δ_t) of BS_i can be obtained:[8] $R = T = 1/2, \cos^2 2\Psi_r = 1/3, \Psi_t = \pi/2 - \Psi_r$, and $(\Delta_r - \Delta_t)$ modulo $\pi = \pi/2$. It has also been noted that optimizing the condition number instead of the determinant results to *similar* optical parameters.[8] Different optical parameters for the diattenuations have been calculated in previous work by optimizing the condition number:[20] $R = T = 1/2, \Psi_r = \pi/8, \Psi_t = \pi/2 - \Psi_r$, and $(\Delta_r - \Delta_t)$ modulo $\pi = \pi/2$. The definition of the condition number has been taken from.[13] In contrast to previous work, we will show that maximizing the absolute value of the determinant is equivalent to minimizing the condition number, while using the same definition of the condition number.[13]

Several beam splitters BS_i have been proposed for the DOAP based on uncoated prisms,[20] coated prisms,[21,22] and interference filters.[23] Interference filters can lead to very good values for determinant of the instrument matrix but only for a limited spectral range. Furthermore, they are also quite expensive.

Recently, we proposed a DOAP with rotating quarter-wave plates.[24,25] Designs of a DOAP with half-wave or quarter-wave plates, one on the reflected and one on the transmitted path, have also been proposed independently in previous work.[26] In that publication, calculations revealed that quarter-wave plates are better suited than half wave plates. Although a DOAP with one wave plate on each path can improve the instrument matrix when $(\Delta_r - \Delta_t)$ modulo $\pi \neq \pi/2$, it does not always lead to an optimal DOAP for all values of $\Delta_r - \Delta_t$, as we have shown previously.[25] In contrast, by using two quarter-wave plates on the same path, an optimal DOAP can be obtained for any value of $\Delta_r - \Delta_t$.[25] In this article, we provide analytic formulas for determining the rotational angles of the retarders depending on the value of $\Delta_r - \Delta_t$. Furthermore, we will present another optimal DOAP with only one quarter-wave plate on the reflected path. To get an optimal DOAP, the rotational angle γ_r of BS_r has to be adjusted depending on $\Delta_r - \Delta_t$.

3. CALCULATION OF THE INSTRUMENT MATRIX

The state of polarization of a plane wave is fully described by the Stokes vector $\boldsymbol{S}$:[15]

$$\boldsymbol{S} = \begin{pmatrix} S_0 \\ S_1 \\ S_2 \\ S_3 \end{pmatrix} = \begin{pmatrix} I_{0^\circ} + I_{90^\circ} \\ I_{0^\circ} - I_{90^\circ} \\ I_{45^\circ} - I_{-45^\circ} \\ I_R - I_L \end{pmatrix} . \tag{1}$$

$I_{0^\circ}, I_{90^\circ}, I_{45^\circ}$, and I_{-45° are the measured intensities of a light wave after passing linear polarizers with azimuthal angles $0^\circ, 90^\circ, 45^\circ$, and -45°, respectively. I_R and I_L are the measured intensities after it passes left and right circular polarizers. Although it is possible to measure the Stokes vector $\boldsymbol{S}$ by six intensities according to Equation (1), only four intensity measurements $\boldsymbol{I} = (I_1, I_2, I_3, I_4)^\intercal$ are necessary which are measured by the photodetectors $D_1, \ldots, D_4$. The instrument matrix $\mathbf{A}$ defines a linear map between $\boldsymbol{S}$ and $\boldsymbol{I}$

$$\begin{pmatrix} I_1 \\ I_2 \\ I_3 \\ I_4 \end{pmatrix} = \mathbf{A} \cdot \begin{pmatrix} S_0 \\ S_1 \\ S_2 \\ S_3 \end{pmatrix} . \tag{2}$$

The sensor model in Equation (2) is a simplification of the real-world scenario. For instance, the quantization of the photodetector signals and the quantum efficiency of the photodetectors have been omitted. The Stokes vector $\boldsymbol{S}$ of the incoming light beam can be calculated from the measured intensities $\boldsymbol{I}$ by inverting Equation (2).

The change of the SOP of a light beam passing through an optical system consisting of n optical components can be described by subsequent linear maps

$$\boldsymbol{S}^{\text{out}} = \underbrace{\mathbf{M}_n \cdot \mathbf{M}_{n-1} \cdot \ldots \cdot \mathbf{M}_1}_{=:\mathbf{M}} \cdot \boldsymbol{S}^{\text{in}}, \tag{3}$$

where $\mathbf{M}_1, \mathbf{M}_2, \ldots, \mathbf{M}_n$ are the Mueller matrices of the optical components. The change of the SOP of a light beam, which is reflected at BS_i and then impinges on BS_r before it is detected by D_1, can be described by the Mueller matrix

$$\mathbf{M}_\text{P}(45°) \cdot \mathbf{M}_\text{S}(\Psi_r, \Delta_r, R), \tag{4}$$

where $\mathbf{M}_\text{P}(\alpha)$ is the Mueller matrix of a polarizer rotated at the azimuthal angle α and $\mathbf{M}_\text{S}(\Psi_r, \Delta_r, R)$ is the Mueller matrix of an ellipsometric surface described by the ellipsometric parameters Ψ_r, Δ_r, and the reflectance R. Let I_1 be the intensity measured by the polarization-insensitive photo-detector D_1 for the previously described light path and let $\boldsymbol{q} := (1, 0, 0, 0)^\intercal$. I_1 is then calculated by:

$$I_1 = \boldsymbol{q} \cdot \mathbf{M}_\text{P}(45°) \cdot \mathbf{M}_\text{S}(\Psi_r, \Delta_r, R) \cdot \boldsymbol{S} \ . \tag{5}$$

By using the corresponding formulas for I_2, I_3, and I_4, we get the following instrument matrix of the DOAP:

$$\mathbf{A} := \begin{pmatrix} \boldsymbol{q}\mathbf{M}_\text{P}(45°)\mathbf{M}_\text{S}(\Psi_r, \Delta_r, R) \\ \boldsymbol{q}\mathbf{M}_\text{P}(-45°)\mathbf{M}_\text{S}(\Psi_r, \Delta_r, R) \\ \boldsymbol{q}\mathbf{M}_\text{P}(45°)\mathbf{M}_\text{S}(\Psi_t, \Delta_t, T) \\ \boldsymbol{q}\mathbf{M}_\text{P}(-45°)\mathbf{M}_\text{S}(\Psi_t, \Delta_t, T) \end{pmatrix} = \frac{1}{2} \begin{pmatrix} R & -R\cos 2\Psi_r & R\cos\Delta_r \sin 2\Psi_r & R\sin\Delta_r \sin 2\Psi_r \\ R & -R\cos 2\Psi_r & -R\cos\Delta_r \sin 2\Psi_r & -R\sin\Delta_r \sin 2\Psi_r \\ T & -T\cos 2\Psi_t & T\cos\Delta_t \sin 2\Psi_t & T\sin\Delta_t \sin 2\Psi_t \\ T & -T\cos 2\Psi_t & -T\cos\Delta_t \sin 2\Psi_t & -T\sin\Delta_t \sin 2\Psi_t \end{pmatrix} . \tag{6}$$

The determinant of $\mathbf{A}$ is given by:[8]

$$\det \mathbf{A} = \frac{1}{4} R^2 T^2 (\cos 2\Psi_r - \cos 2\Psi_t) \sin 2\Psi_r \sin 2\Psi_t \sin(\Delta_r - \Delta_t) \ . \tag{7}$$

Maximizing $|\det \mathbf{A}|$ leads to the following optimal optical parameters of BS_i:[8]

$$R^* = T^* = \frac{1}{2}, (\Delta_r^* - \Delta_t^*) \text{ modulo } \pi = \frac{\pi}{2}, \Psi_r^* = \frac{1}{2}\arccos(\pm 1/\sqrt{3}), \Psi_t^* = \frac{\pi}{2} - \Psi_r^* \ . \tag{8}$$

The resulting instrument matrix will be denoted as $\mathbf{A}_\text{DOAP}$ and the following holds:

$$\det_\text{max} := \max_{\mathbf{A}} |\det \mathbf{A}| = |\det \mathbf{A}_\text{DOAP}| = \sqrt{3}/144 \approx 0.012 \ . \tag{9}$$

To measure how close alternative designs of the DOAP reach the optimal value, the normalized determinant is defined as follows:[22]

$$|\det \mathbf{A}|_\text{norm} := \frac{|\det \mathbf{A}|}{\det_\text{max}} \ . \tag{10}$$

Furthermore, we define the condition number of a non-singular instrument matrix $\mathbf{A}$ as follows:[12]

$$\text{cond}(\mathbf{A}) = \frac{\sigma_\text{max}}{\sigma_\text{min}}, \tag{11}$$

where σ_max and σ_min are the maximum and minimum singular values of $\mathbf{A}$, respectively. Although we did not find a closed form for Equation (11) in order to calculate the minimum, numerical simulations reveal that the optimal condition number has the following value which is consistent with previous work:[12,13,27]

$$\text{cond}_\text{min} := \min_{\mathbf{A}} \text{cond}(\mathbf{A}) = \text{cond}(\mathbf{A}_\text{DOAP}) = \sqrt{3} \approx 1.732 \ . \tag{12}$$

Analogous to Equation (10), we define the normalized condition number as:

$$\mathrm{cond}_{\mathrm{norm}}(\mathbf{A}) = \frac{\mathrm{cond}_{\mathrm{min}}}{\mathrm{cond}(\mathbf{A})} \ . \tag{13}$$

From Equation (9) and Equation (12) we get:

$$|\det \mathbf{A}_{\mathrm{DOAP}}|_{\mathrm{norm}} = \mathrm{cond}_{\mathrm{norm}}(\mathbf{A}_{\mathrm{DOAP}}) = 1 \ . \tag{14}$$

In previous work it has been stated that the optimal values for $\mathrm{BS_i}$ minimizing the condition number are:[20]

$$R = T = 1/2, (\Delta_r - \Delta_t) \text{ modulo } \pi = \frac{\pi}{2}, \Psi_r = \pi/8, \Psi_t = \frac{\pi}{2} - \Psi_r \ . \tag{15}$$

We denote the resulting instrument matrix as $\mathbf{A}^C_{\mathrm{DOAP}}$. To calculate the optimal values in Equation (15), an alternative definition of the condition number has been used:

$$\mathrm{cond}^{\mathrm{C}}(\mathbf{A}) = \sqrt{\frac{\lambda^C_{\mathrm{max}}}{\lambda^C_{\mathrm{min}}}}, \tag{16}$$

where λ^C_{max} and λ^C_{min} are the maximum and minimum eigenvalues of the symmetric matrix $\mathbf{A}^\intercal\mathbf{A}$, respectively. However, both definitions of the condition number lead to the same values

$$\mathrm{cond}(\mathbf{A}_{\mathrm{DOAP}}) = \mathrm{cond}^{\mathrm{C}}(\mathbf{A}_{\mathrm{DOAP}}) = \sqrt{3}, \tag{17}$$

$$\mathrm{cond}(\mathbf{A}^C_{\mathrm{DOAP}}) = \mathrm{cond}^{\mathrm{C}}(\mathbf{A}^C_{\mathrm{DOAP}}) = 2, \tag{18}$$

which means that $\mathbf{A}_{\mathrm{DOAP}}$ is better than $\mathbf{A}^C_{\mathrm{DOAP}}$ independent which definition is used. Furthermore, it has been stated that the two conditions are not fulfilled simultaneously.[13] As we have shown in Equation (14), this is not true. It can be summarized that the optimal values for $\mathrm{BS_i}$ from Equation (8) simultaneously maximize $\mathrm{cond}_{\mathrm{norm}}(\mathbf{A})$, leading to a minimum relative error,[13] and minimize $|\det \mathbf{A}|_{\mathrm{norm}}$, leading to a minimum absolute error.[8] Furthermore, the optimization of $|\det \mathbf{A}|_{\mathrm{norm}}$ and $\mathrm{cond}_{\mathrm{norm}}(\mathbf{A})$ does not lead to similar[8] but equal results. It should be noted that the optimal parameters found by maximizing $|\det \mathbf{A}|_{\mathrm{norm}}$ or $\mathrm{cond}_{\mathrm{norm}}(\mathbf{A})$ are only equal if $|\det \mathbf{A}|_{\mathrm{norm}} = 1$. If there is no parameter set satisfying $|\det \mathbf{A}|_{\mathrm{norm}} = 1$, it is possible that the optimum of $|\det \mathbf{A}|_{\mathrm{norm}}$ and $\mathrm{cond}_{\mathrm{norm}}(\mathbf{A})$ correspond to different parameters.

4. DOAP WITH RETARDERS

A design of the DOAP with two rotated quarter-wave plates is shown in Figure 2 where β_r and β'_r are the azimuthal angles of the quarter-wave plates. Let $\mathbf{M}_{\mathrm{Q}}(\alpha)$ be the Mueller matrix of a quarter-wave plate with the fast axis at the azimuthal angle α. As mentioned previously, a quarter-wave plate with high transmission has nearly a theoretical optimal Mueller matrix:

$$\mathbf{M}_{\mathrm{Q}}(0°) = \begin{pmatrix} 1 & 0 & 0 & 0 \\ 0 & 1 & 0 & 0 \\ 0 & 0 & 0 & 1 \\ 0 & 0 & -1 & 0 \end{pmatrix} \ . \tag{19}$$

Let $\mathbf{A}_{2Q_r}(\Delta_r, \Delta_t, \beta_r, \beta'_r)$ be the instrument matrix of the aforementioned DOAP with two retarders, where R, T, Ψ_r, and Ψ_t are optimal (according to Equation (8)) but Δ_r and Δ_t are not:

$$\mathbf{A}_{2\mathrm{Q}}(\Delta_r, \Delta_t, \beta_r, \beta'_r) = \begin{pmatrix} \boldsymbol{q}\mathbf{M}_{\mathrm{P}}(45°)\mathbf{M}_{\mathrm{Q}}(\beta'_r)\mathbf{M}_{\mathrm{Q}}(\beta_r)\mathbf{M}_{\mathrm{S}}(\Psi^*_r, \Delta_r, R^*) \\ \boldsymbol{q}\mathbf{M}_{\mathrm{P}}(-45°)\mathbf{M}_{\mathrm{Q}}(\beta'_r)\mathbf{M}_{\mathrm{Q}}(\beta_r) \cdot \mathbf{M}_{\mathrm{S}}(\Psi^*_r, \Delta_r, R^*) \\ \boldsymbol{q}\mathbf{M}_{\mathrm{P}}(45°)\mathbf{M}_{\mathrm{S}}(\Psi^*_t, \Delta_t, T^*) \\ \boldsymbol{q}\mathbf{M}_{\mathrm{P}}(-45°)\mathbf{M}_{\mathrm{S}}(\Psi^*_t, \Delta_t, T^*) \end{pmatrix} \ . \tag{20}$$

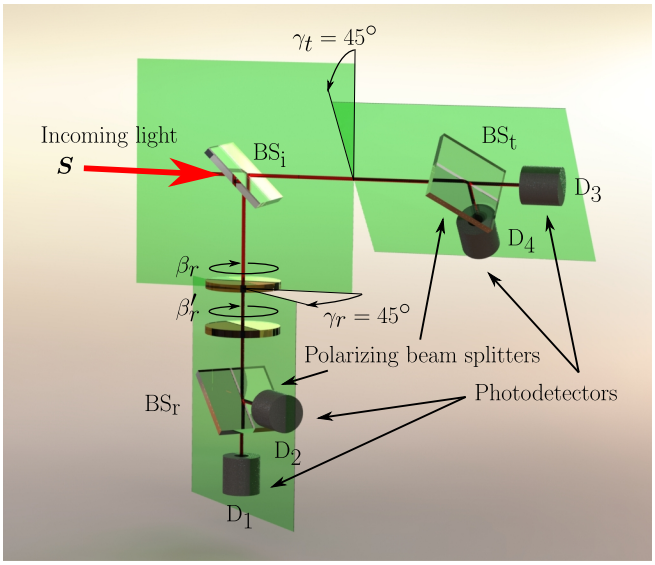

Figure 2. DOAP with two quarter-wave plates mounted at the reflected path

For any value of Δ_r and Δ_t, we can achieve $|\det \mathbf{A}_{2Q}(\Delta_r, \Delta_t, \beta_r, \beta'_r)|_{\text{norm}} = \text{cond}_{\text{norm}}(\mathbf{A}_{2Q}(\Delta_r, \Delta_t, \beta_r, \beta'_r)) = 1$ by using the following formula for β_r and β'_r:

$$\beta_r = \frac{\sec^{-1} A + \sec^{-1} B}{2}, \tag{21}$$

$$\beta'_r = \frac{\csc^{-1} A + \csc^{-1} B}{2}, \tag{22}$$

$$A = \frac{2}{\sqrt{\left(1 - \sqrt{\sin^2 z + 2\sin z \cos 2z + 1}\right) \csc z + 3}},$$

$$B = \frac{4(\sin z + 1)\cos z}{\left(2\sin z + \cos 2z + \sqrt{-4\sin z + 4\sin 3z - 2\cos 2z + 6} - 1\right)\sqrt{\left(1 - \sqrt{-\sin z + \sin 3z - \frac{1}{2}\cos 2z + \frac{3}{2}}\right)\csc z + 3}},$$

$$z = ((\Delta_r - \Delta_t + \pi/2) \text{ modulo } \pi) - \pi/2 \ .$$

Figure 3 show the azimuthal angles β_r and β'_r resulting from Equation (21) and (22) depending on the values of Δ_r and Δ_t.

There is another possibility not mentioned in previous work to get an optimal DOAP with only one quarter-wave plate: The quarte-wave plate is mounted at the reflected path at the fixed azimuthal angle $\beta_r = 45°$. To get an optimal DOAP, the azimuthal angle of BS_r has to be adjusted, while the azimuthal angle of BS_t remains unchanged $\gamma_t = 45°$. Adjusting γ_r using the following formula also gives $|\det \mathbf{A}|_{\text{norm}} = \text{cond}_{\text{norm}}(\mathbf{A}) = 1$:

$$\gamma_r = \frac{\Delta_t - \Delta_r}{2} \ . \tag{23}$$

It should be mentioned that adjusting the azimuthal angles according to Equation (21), (22), and (23) not only improves $|\det \mathbf{A}|_{\text{norm}}$ for optimal values of R, T, Ψ_r, and Ψ_t but for any values. The factorization of $\det \mathbf{A}$ in Equation (7) means that the optimization of R, T, Ψ_r, and Ψ_t is independent from the optimization of Δ_r and Δ_t. The latter can be achieved by improving the beam splitter or by using the proposed designs with quarter-wave plates. Finally, BS_i should be a non-absorbing beam splitter with $R + T = 1$ to get a low measurement error. In

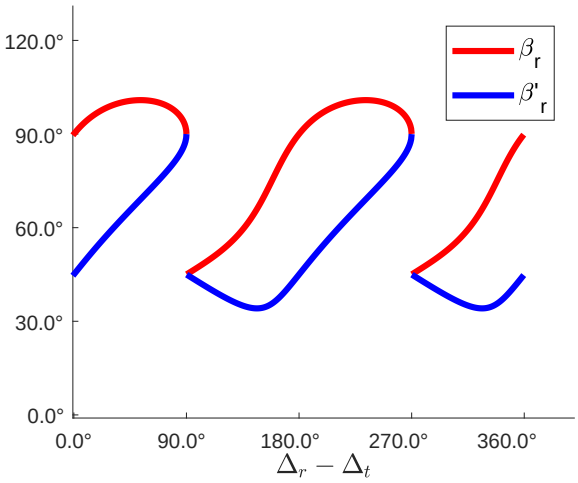

Figure 3. Azimuthal angles β_r and β'_r of the quarter-wave plates leading to an optimal DOAP.

this case, only the reflectance for the $p-$ and $s-$polarization, R^p and R^s, has to be optimal:

$$R^s = \frac{1}{6}(3 \pm \sqrt{3}),$$
$$R^p = 1 - R^s \ . \tag{24}$$

The other conditions $R = T = 1/2, \cos^2 2\Psi_r = \frac{1}{3}$, and $\Psi_t = \frac{\pi}{2} - \Psi_r$ follow directly from Equation (24).

5. EXPERIMENTAL SIMULATIONS

A DOAP with a prism made of a low-refractive-index coating on a high-refractive-index substrate (MgF_2 on ZnS (Cleartran)) has been proposed in previous work.[21] The refractive index of the coating is $n_F = 1.38$ and the refractive index of the substrate is $n_S = 2.3$ at $\lambda = 632.8\,\text{nm}$. For further examination we will just use the prism substrate without the coating, as a coating enhances the variation of the optical parameters in a broad wavelength range. It has turned out that high-refractive-index materials are well suited to get optimal values for R^p and R^s according to Equation (24). The optimal angle of incidence of the incoming light impinging the surface of the prism is $\theta = 82°$. From θ we get the following angles describing the geometry of the prism: $\alpha = 25.2°, \beta = 90°$, and $\gamma = 64.8°$. It is assumed that the prism has an anti-reflection coating on the exit surface of the transmitted beam to avoid an intensity loss. Anti-reflection coatings do not change the state of polarization at normal incidence. A suitable coating for monochromatic measurement ($\lambda = 632.8\,\text{nm}$) would be e.g. a glass with a refractive index of $n_F = 1.53$ and a thickness of $d = 67.2\,\text{nm}$. For broadband application a broadband anti-reflection coating would be necessary. Furthermore, it is assumed that the Mueller-matrix of the quarter-wave plate is constant for all wavelengths (according to Equation (19)). A Fresnel rhomb with anti-reflection coatings on the entrance and exit surface are a good approximation for this assumption. The Fresnel rhomb can be mounted at the reflected path rotated at $\beta_r = 0°$ to fulfill $\Delta_r - \Delta_t = \pi/2$. Figure 4 shows the values of the normalized determinant and condition number obtained with the proposed setup for $\lambda \in [400\,\text{nm}, 1000\,\text{nm}]$. The values have been calculated with Mathematica and Matlab using the plane-wave approximation and assuming the mentioned ideal optical components with ideal (broadband) anti-reflection coatings. In order to verify the calculations, the physical optics software VirtualLab Fusion from LightTrans has been used to simulate measurements with the DOAP including a model of the proposed beam splitter with the aforementioned single-layer anti-reflection coating. A right-handed circularly polarized, monochromatic ($\lambda = 632.8\,\text{nm}$) Gaussian beam with a waist radius of $100\,\mu\text{m}$ has been propagated through the DOAP by using the "2^{nd} generation field tracing" feature of VirtualLab Fusion.

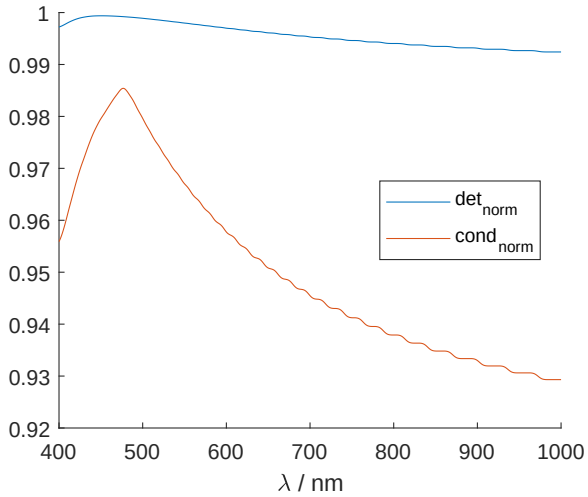

Figure 4. Normalized determinant and condition number obtained with a high-refractive-index prism.

The following intensity vectors have been obtained with the simulation in VirtualLab Fusion and Matlab:

$$\boldsymbol{I}_{\mathrm{V}} = \begin{pmatrix} 0.444 & 0.000 & 0.247 & 0.247 \end{pmatrix}^{\intercal}, \tag{25}$$

$$\boldsymbol{I}_{\mathrm{M}} = \begin{pmatrix} 0.452 & 0.041 & 0.253 & 0.253 \end{pmatrix}^{\intercal}, \tag{26}$$

where $\boldsymbol{I}_{\mathrm{V}}$ and $\boldsymbol{I}_{\mathrm{M}}$ are the calculated intensities with VirtualLab Fusion and Matlab, respectively. Although there are small deviations, the values are comparable and the calculations plausible.

6. SUMMARY AND OUTLOOK

In this article we proposed a simplification of previous designs of a DOAP for measuring the SOP of a light beam. A critical component of the DOAP is the first beam splitter, which splits up the incoming beam into two beams. To get a low measurement error, the reflectance, transmittance, diattenuation and retardance of the beam splitter need to be optimal. Using additional quarter-wave plates relaxes the constraint on the retardance. This provides an additional degree of freedom when designing the beam splitter. For example, reflection and refraction at dielectrics usually results into a retardance of 0° or 180° but for a DOAP without retarders a retardance of 90° is required. We presented a DOAP consisting of two quarter-wave plates mounted at the reflected path and provided analytic formulas to calculate the azimuthal angles. It can been shown that this design is better than mounting one quarter-wave plate at each path, because the negative effect resulting from beam splitters with suboptimal retardances can always be compensated. A similar design with only one quarter-wave plate has also been provided. Furthermore, simulations revealed that if the normalized determinant is equal to one, the same holds for the normalized condition number, and vice versa. As a consequence, the absolute and relative measurement errors are minimized simultaneously at an optimal DOAP. Additionally, we presented the optical setup of a DOAP consisting of a special beam-splitter prism, which is suitable for broadband application resulting into a normalized determinant greater than 0.99 from $\lambda \in [400\,\mathrm{nm} - 1000\,\mathrm{nm}]$. For the best of our knowledge, previous designs of the DOAP achieve a normalized determinant greater than 0.99 only for a narrow wavelength range. Other proposed designs used for broadband application do not reach such a high value for the normalized determinant. We assumed that a perfect achromatic quarter-wave retarder with appropriate (broadband) anti-reflection coatings is available. To simulate the measurement of a monochromatic Gaussian beam with the DOAP consisting of the proposed beam splitter prism, the physical optics simulation software VirtualLab Fusion has been used. The results are comparable to the calculations performed in Mathematica and Matlab using the plane-wave approximation. Further simulations are planned to simulate the calibration and measurement of the DOAP for the whole spectral range and to simulate a realistic model of the achromatic retarder with appropriate broadband anti-reflection coatings.

REFERENCES

[1] Meriaudeau, F., Ferraton, M., Stolz, C., Morel, O., and Bigué, L., "Polarization imaging for industrial inspection," in [*Image Processing: Machine Vision Applications*], Niel, K. S. and Fofi, D., eds., *SPIE Proceedings*, 681308, SPIE (2008).

[2] Wolff, L. B., "Polarization-based material classification from specular reflection," *IEEE Transactions on Pattern Analysis and Machine Intelligence* **12**(11), 1059–1071 (1990).

[3] Morel, O., Ferraton, M., Stolz, C., and Gorria, P., "Active lighting applied to shape from polarization," in [*IEEE International Conference on Image Processing, 2006*], 2181–2184, IEEE Operations Center, Piscataway, NJ (2006).

[4] Canillas, A., Polo, M. C., Andújar, J. L., Sancho, J., Bosch, S., Robertson, J., and Milne, W. I., "Spectroscopic ellipsometric study of tetrahedral amorphous carbon films: optical properties and modelling," *Diamond and Related Materials* **10**(3-7), 1132–1136 (2001).

[5] Cui, Y. and Azzam, R. M., "Applications of the normal-incidence rotating-sample ellipsometer to high- and low-spatial-frequency gratings," *Applied optics* **35**(13), 2235–2238 (1996).

[6] Han, C.-Y., Lee, Z.-Y., and Chao, Y.-F., "Determining thickness of films on a curved substrate by use of ellipsometric measurements," *Applied Optics* **48**(17), 3139 (2009).

[7] Azzam, R. M. A., "Division-of-amplitude Photopolarimeter (DOAP) for the Simultaneous Measurement of All Four Stokes Parameters of Light," *Optica Acta: International Journal of Optics* **29**(5), 685–689 (1982).

[8] Azzam, R. M. A. and De, A., "Optimal beam splitters for the division-of-amplitude photopolarimeter," *Journal of the Optical Society of America A* **20**(5), 955 (2003).

[9] Collett, E., "Determination of the ellipsometric characteristics of optical surfaces using nanosecond laser pulses," *Surface Science* **96**(1-3), 156–167 (1980).

[10] Azzam, R. M. A., Masetti, E., Elminyawi, I. M., and Grosz, F. G., "Construction, calibration, and testing of a four–detector photopolarimeter," *Review of Scientific Instruments* **59**(1), 84–88 (1988).

[11] Sabatke, D. S., Descour, M. R., Dereniak, E. L., Sweatt, W. C., Kemme, S. A., and Phipps, G. S., "Optimization of retardance for a complete stokes polarimeter," *Optics Letters* **25**(11), 802 (2000).

[12] Peinado, A., Lizana, A., Vidal, J., Iemmi, C., and Campos, J., "Optimization and performance criteria of a stokes polarimeter based on two variable retarders," *Optics express* **18**(10), 9815–9830 (2010).

[13] Brudzewski, K., "Static stokes ellipsometer: General analysis and optimization," *Journal of Modern Optics* **38**(5), 889–896 (1991).

[14] Azzam, R. M. A.-G. and Bashara, N. M., [*Ellipsometry and polarized light*], North-Holland personal library, Elsevier, Amsterdam, 4. impression, paperback ed. ed. (1999).

[15] Fujiwara, H., [*Spectroscopic ellipsometry: Principles and applications*], John Wiley & Sons, Chichester and England and Hoboken and NJ (2007).

[16] Hauge, P. S., Muller, R. H., and Smith, C. G., "Conventions and formulas for using the Mueller-Stokes calculus in ellipsometry," *Surface Science* **96**(1-3), 81–107 (1980).

[17] Hecht, E., [*Optics*], Addison-Wesley, Reading and Mass, 4th ed ed. (2002).

[18] Beyerer, J., Puente León, F., and Frese, C., [*Automatische Sichtprüfung: Grundlagen, Methoden und Praxis der Bildgewinnung und Bildauswertung*], Springer Vieweg, Berlin and Heidelberg, 2., erweiterte und verbesserte auflage ed. (2016).

[19] Mu, T., Chen, Z., Zhang, C., and Liang, R., "Optimal configurations of full-stokes polarimeter with immunity to both poisson and gaussian noise," *Journal of Optics* **18**(5), 055702 (2016).

[20] Compain, E., Poirier, S., and Drevillon, B., "General and self-consistent method for the calibration of polarization modulators, polarimeters, and mueller-matrix ellipsometers," *Appl. Opt.* **38**, 3490–3502 (Jun 1999).

[21] Azzam, R., "Beam-splitters for the division-of-amplitude photopolarimeter," *Optica Acta: International Journal of Optics* **32**(11), 1407–1412 (1985).

[22] Azzam, R. M. A. and Sudradjat, F. F., "Single-layer-coated beam splitters for the division-of-amplitude photopolarimeter," *Applied Optics* **44**(2), 190 (2005).

[23] Yuan, W., Shen, W., Zhang, Y., and Liu, X., "Dielectric multilayer beam splitter with differential phase shift on transmission and reflection for division-of-amplitude photopolarimeter," *Optics Express* **22**(9), 11011 (2014).

[24] Negara, C., "Fast polarization state detection by division-of-amplitude in a simple configuration setup," in [*Proceedings of the 2015 Joint Workshop of Fraunhofer IOSB and Institute for Anthropomatics, Vision and Fusion Laboratory*], *Karlsruher Schriften zur Anthropomatik ; 24*, 75–89, KIT Scientific Publishing, Karlsruhe (2016).

[25] Negara, C., "Different designs for a polarization state detector based on division-of-amplitude," in [*Proceedings of the 2016 Joint Workshop of Fraunhofer IOSB and Institute for Anthropomatics, Vision and Fusion Laboratory*], Beyerer, J. and Pak, A., eds., 85–107, KIT Scientific Publishing (2017).

[26] Zeng, L., Cai, Y., Tan, C., and Huang, Z., "Optimization of stokes optical polarization measurement system," *Laser Technology* **41**(1), 74 (2017). (Chinese).

[27] Tyo, J. S., "Noise equalization in stokes parameter images obtained by use of variable-retardance polarimeters," *Optics Letters* **25**(16), 1198 (2000).